Arch Virol (2015) 160:649–662
DOI 10.1007/s00705-014-2309-7

ORIGINAL ARTICLE

The gene expression profile of porcine alveolar macrophages infected with a highly pathogenic porcine reproductive and respiratory syndrome virus indicates overstimulation of the innate immune system by the virus

Yan Xiao · Tong-Qing An · Zhi-Jun Tian · Tian-Chao Wei · Yi-Feng Jiang · Jin-Mei Peng · Yan-Jun Zhou · Xue-Hui Cai · Guang-Zhi Tong

Received: 19 August 2014 / Accepted: 3 December 2014 / Published online: 12 December 2014

Abstract Since the highly pathogenic porcine reproductive and respiratory syndrome virus (HP-PRRSV) variant emerged in 2006, it has caused death in more than 20 million pigs in China and other Southeast Asian countries, making it the most destructive swine pathogen currently in existence. To characterize the cellular responses to HP-PRRSV infection, the gene expression profile of porcine alveolar macrophage (PAM) cells, the primary target cells of PRRSV, was analyzed in HP-PRRSV-infected and uninfected PAMs by suppression subtractive hybridization. After confirmation by Southern blot, genes that were differentially expressed in the HP-PRRSV-infected and uninfected PAMs were sequenced and annotated. Genes that were upregulated mainly in HP-PRRSV-infected PAM cells were related to immunity and cell signaling. Among the differentially expressed genes, Mx1 and HSP70 protein expression was confirmed by western blotting, and IL-8 expression was confirmed by ELISA. In PAM cells isolated from HP-PRRSV-infected piglets, the differential expression of 21 genes, including IL-16, TGF-beta type 1 receptor, epidermal growth factor, MHC-I SLA, Toll-like receptor, hepatoma-derived growth factor, FTH1, and MHC-II SLA-DRB1, was confirmed by real-time PCR. To our knowledge, this is the first study to demonstrate differential gene expression between HP-PRRSV-infected and uninfected PAMs *in vivo*. The results indicate that HP-PRRSV infection excessively stimulates genes involved in the innate immune response, including proinflammatory cytokines and chemokines.

Y. Xiao · T.-Q. An (✉) · Z.-J. Tian · T.-C. Wei · Y.-F. Jiang · J.-M. Peng · Y.-J. Zhou · X.-H. Cai · G.-Z. Tong
State Key Laboratory of Veterinary Biotechnology, Harbin Veterinary Research Institute, CAAS, No. 427 Maduan Street, Nangang District, Harbin 150001, China
e-mail: antongqing@163.com

G.-Z. Tong (✉)
Shanghai Veterinary Research Institute, CAAS, No. 518 Ziyue Road, Minhang District, Shanghai 200241, China
e-mail: gztong@shvri.ac.cn

Introduction

Porcine reproductive and respiratory syndrome (PRRS), characterized by reproductive failure in pregnant sows and respiratory distress in pigs of all ages, continues to be one of the most economically devastating diseases in the pig farming industry worldwide since it emerged in North America in 1987 [16]. PRRS virus (PRRSV), the causative agent [22] of the disease, is an enveloped virus containing a 15.4-kb positive-strand RNA genome [23] and is a member of the family *Arteriviridae* within the order *Nidovirales* [3]. The viral genome contains the following nine open reading frames (ORFs): ORF1a and ORF1b encode viral replicase polyproteins, while ORF2a, ORF2b, and ORFs 3–7 encode the viral structural proteins GP2, E, GP3, GP4, GP5, M, and N, respectively [23, 33, 38]. There are two PRRSV genotypes: North American and European (NA-type and EU-type, respectively) [27].

In April 2006, a highly pathogenic PRRSV (HP-PRRSV) emerged in China and spread quickly throughout most of its provinces. Infection with this virus led to high fever, high morbidity (50–100 %), and high mortality (20–100 %) in pigs of all ages and caused more than two million deaths [34, 35]. HP-PRRSV also affected pigs in Vietnam, Thailand, and some other Southeast Asian countries [1], causing great concern to the global swine industry. The molecular mechanism underlying the significantly enhanced pathogenicity of HP-PRRSV compared

with the classical PRRSV isolated in China before 2006 remains elusive.

Macrophages, as important components of the innate immune system, play key roles in clearing microbial pathogens and maintaining host homeostasis through their scavenger-like abilities. During a viral infection, specialized proteins expressed by host cells recognize viral nucleic acids or proteins, thereby triggering signaling pathways within the infected cell. PRRSV has a strict tropism for cells of the monocyte/macrophage lineage. Lung-resident porcine alveolar macrophages (PAMs) are the primary target cells for PRRSV infection *in vivo* [32], although macrophages isolated from the spleen, tonsils, lymph nodes, and thymus can also support productive PRRSV replication [9, 36]. Because of the importance of PAM-PRRSV interactions during PRRSV infections, investigating PAM responses may help to unravel how HP-PRRSV causes increased pathogenicity of the virus in pigs. In particular, we hypothesize that investigating which PAM genes are differentially expressed before and during infection with HP-PRRSV might help us to learn more about the molecular basis of the disease. Genini et al. previously evaluated the gene expression profile of innate immune genes from PAMs infected *in vitro* with the European PRRSV Lelystad strain using a porcine Chip microarray and showed that a few innate immune genes were upregulated, including the antiviral cytokine type I IFN-β gene [10]. Because the biological effects of the European strains are distinct from those of the North American isolates, in a separate study, the transcriptomic changes in PAMs infected with the North American PRRSV VR2332 strain were also evaluated using serial analysis of gene expression methodology, and very little or no change was observed in the innate immune genes at any time point following infection [25]. However, no study has included a comprehensive analysis of the innate immune changes induced specifically within PAM cells upon infection with the highly pathogenic strain.

In this study, we constructed two cDNA libraries and used the suppression subtractive hybridization (SSH) method to investigate differentially expressed genes in HP-PRRSV-infected or uninfected PAM cells and identified some differentially expressed genes *in vitro* and *in vivo*.

Materials and methods

Ethics statement

Animal experiments were approved by the Harbin Veterinary Research Institute of the Chinese Academy of Agricultural Sciences. All procedures were conducted in accordance with animal ethics guidelines and approved protocols. The Animal Ethics Committee approval number is Heilongjiang-SYXK 2006-032.

Cells and virus

PAMs were obtained under sterile conditions from 6-week-old PRRS antibody- and virus-negative Large White/Landrace cross piglets as described previously [12, 37]. The cells were cultivated in RPMI 1640 medium supplemented with 10 % fetal bovine serum (Gibco BRL, Gaithersburg MD, USA) and 100 IU of penicillin and 100 mg of streptomycin per mL in a humidified 5 % CO_2 atmosphere at 37 °C. The HP-PRRSV strain HuN4 (GenBank no. EF635006), isolated in 2006 in China, was maintained in our laboratory and was confirmed to be highly pathogenic to piglets [35].

Construction of the SSH cDNA library

To determine the appropriate time point for extraction of cellular RNA, we investigated the replication kinetics of HP-PRRSV in PAM cells using PRRSV-specific quantitative real-time RT-PCR. The primers and probe (forward, 5′-AAATACAACGGCAAGCAGC-3′; reverse, 5′-AGACACAATTGCCGCTCACTA-3′; probe, FAM-CAAAACCAGTCCAGAGGCAAGGG-BHQ1) correspond to the conserved region of the PRRSV ORF7 gene. PAM cells were freshly obtained from a donor pig, seeded onto a six-well plate, and allowed to adsorb to the plate at 37 °C for 8 hours. The cells were then infected with the HuN4 virus at a titer of 1000 copies/well. As an uninfected control, cells were mock treated with sterile PBS and processed exactly like the infected cells. Cells were harvested for RNA extraction every 12 hours from 0 to 96 hours post-infection (hpi) from both the uninfected control and the PRRSV-infected cultures. Real-time RT-PCR was performed using an Mx3000P Real-Time PCR System (Genetimes Technology Inc.). The total volume of each reaction was 25 μL, and the concentration of each primer was 100 nM. A hot-start enzyme was used with the following PCR conditions: 50 °C for 2 min, 95 °C for 10 min, and 40 cycles of 94 °C for 30 s, 53 °C for 1 min, and 72 °C for 30 s.

Total RNA from HP-PRRSV-HuN4-infected or control PAM cells at 40 hpi (just before the peak of viral replication at 48 hpi) were extracted using an RNeasy Plus Mini Kit (QIAGEN, Valencia, CA). cDNA libraries were constructed by SSH using a PCR-Select^{TM} cDNA Subtraction Kit (Clontech, USA) following the manufacturer's protocol. Briefly, mRNA (2 μg) from control or HP-PRRSV-infected cells was reverse transcribed into cDNA. For the forward subtraction, cDNA from the control cells was used as the driver, and cDNA from the

HP-PRRSV-infected cells was used as the tester for identifying upregulated gene expression. For the reverse subtraction, cDNA from the control or HP-PRRSV-infected cells was applied as the tester and the driver, respectively, to detect downregulated gene expression. All procedures, including cDNA synthesis, *Rsa* I digestion, adaptor ligation, first and second hybridizations, and first and second PCR amplifications, were performed according to manufacturer's instructions. The PCR products obtained from both the forward and reverse subtractions were cloned separately into a pGEM-T vector (Promega) and then used to transform *E. coli* DH5α cells to establish different cDNA libraries. The transformed bacteria were plated onto Luria-Bertani (LB) agar plates containing ampicillin, isopropyl-β-D-thiogalactopyranoside and X-gal. After overnight incubation at 37 °C, recombinant white colonies were randomly selected and cultured in LB broth containing ampicillin, followed by PCR identification.

Screening cDNA libraries by Southern blot analysis

Approximately 600 individual recombinant clones were randomly chosen, and each individual clone was PCR amplified using the same nested primers, followed by analysis on a 2 % agarose gel. PCR products over 100 bp were selected, and 200 individual clones from each library were analyzed by Southern blotting. Each sample from the forward- or reverse-subtracted cDNA libraries was spotted onto two nylon membranes, one for each membrane, in the same position. The avian reticuloendotheliosis virus (REV) gp90 gene acted as a non-porcine-derived control. For denaturing purposes, each kit-purified (Watson, Shanghai, China) PCR product was mixed with the same volume of 0.6 N NaOH, denatured for 10 min at 100 °C, and then chilled on ice. Each denatured product was individually blotted onto a Nytran® nylon membrane (Schleicher Schuell, Keene, NH) in duplicate and fixed. DIG-labeled cDNA probes from either the forward or reverse subtractions were prepared separately using a DIG Random Labeling and Detection Kit II (Jishide, Wuhan, China) according to the manufacturer's protocol. The duplicate membranes were then hybridized with either of the two probes, and the gray density on the hybrid membranes was measured. Densitometry scanning with a Disk Scanning Biological Fluorescent Microscope (Olympus IX2-DSU) followed by analysis with Image-Pro Plus 5.0 software (Media Cybernetics, USA) was used to quantify the density value of each sample dot. Samples hybridized to the tester probe exhibiting values of two-fold or greater over the control as determined by densitometry were considered positive and were selected for further analysis.

DNA sequencing and gene annotation

Positive samples from the Southern blot analysis were sequenced using an ABI PRISM 3370 DNA Sequencer at Invitrogen Inc. (Shanghai, China). The sequences generated were subjected to Basic Local Alignment Search Tool (BLAST) analysis using various online databases to identify the clones, as described previously [11]. These databases included the National Center for Biotechnology Information nonredundant (NR) database (NR GenBank, EMBL, DDBJ, and PDB) and the EST database (NR GenBank, EMBL, and DDBJ EST divisions). Clone redundancy was determined by sequence alignment using Lasergene software (DNASTAR, Madison, WI). Classification of gene function was done using the DAVID bioinformatics resource [8, 13, 14], and gene interactions were analyzed using Cytoscape software [6].

IL-8 quantification by ELISA

For quantitative determination of IL-8, the cell culture medium from HP-PRRSV-HuN4-infected or noninfected PAM cells was collected at 6, 24, 48, and 72 hpi. IL-8 was detected using a commercial swine IL-8 ELISA kit (Invitrogen) according to the manufacturer's instructions. The absorbance was read at 450 nm. The process was repeated three times. Data were analyzed using unpaired Student's *t*-tests and expressed as the mean ± SD (pg/mL).

Identification of Mx1 and HSP70 by western blot

Western blot analysis of Mx1 or HSP70 protein was carried out using PRRSV-infected PAM cells. The cells were harvested using lysis buffer containing 150 mM NaCl, 1 mM $CaCl_2$, 25 mM Tris-HCl (pH 7.4), and 1 % Triton-X-100 supplemented with a protease inhibitor cocktail (Sigma). Total cell extracts (50 μg per lane) were separated on a 12 % SDS polyacrylamide gel and transferred onto a PVDF membrane. The Mx1 protein was visualized with a polyclonal goat anti-Mx1 antibody (Santa Cruz Biotechnology, Santa Cruz, CA) at a 1:1000 dilution, and the HSP70 protein was visualized with a mouse anti-HSP70 monoclonal antibody (Abcam) at a 1:100 dilution. Antibody–antigen complexes were detected with horseradish peroxidase-labeled rabbit anti-goat IgG (Sigma) at a 1:8000 dilution. β-actin was detected with an anti-β-actin antibody (Sigma) at a 1:5000 dilution, and the bound antibodies were detected with horseradish-peroxidase-labeled goat anti-mouse IgG (Sigma) at a 1:5000 dilution. The membranes were incubated with ECL Western Blotting Substrate (Pierce, Rockford, IL, USA) and analyzed using the ImageQuant 350 imaging system (GE Healthcare).

mRNA analysis of differentially expressed genes in infected piglets

Fifteen 6-week-old PRRS-antibody-negative and PRRSV-negative pigs were randomly divided into two groups. Pigs in group 1 (n = 6) were inoculated intramuscularly (1 mL) and intranasally (2 mL) with the PRRSV HuN4 strain ($3 \times 10^{4.0}$ $TCID_{50}$ per pig). Uninfected control pigs in group 2 (n = 9) were inoculated by the same routes with the same volumes of Dulbecco's minimal essential medium (Gibco BRL, Gaithersburg MD, USA). Animals were kept in Biosafety Level 2 conditions and housed separately. Clinical symptoms of infection, including reduced appetite, coughing, and respiratory distress, were recorded daily, as were rectal temperatures. Serum samples were collected at 0, 3, 5, 7, 11, and 14 days postinfection (dpi) and were used to detect viral titers by real-time RT-PCR as described above.

To obtain PAM cells from infected piglets, the piglets were euthanized at different dpi. In the infected group (n = 6), three piglets were euthanized at 7 dpi, and the remaining three at 14 dpi. In the uninfected group (n = 9), the piglets were euthanized at 0 dpi, 7 dpi and 14 dpi, respectively, using three piglets for each time point. The right lung of each pig was used to prepare PAM cells to detect up- and downregulated genes. The left lungs were harvested, fixed in 10 % neutral-buffered formalin, and routinely processed for histological examination.

The mRNA expression levels of differentially expressed genes were analyzed by real-time RT-PCR. PAM RNA was extracted and reverse transcribed into cDNA using oligo(dT) primers and a commercial Primescript RT reagent kit (TaKaRa, Dalian, China). RNA expression was quantified using a Perfect Real Time quantitative RT-PCR kit (Takara) according to the manufacturer's instructions. For each gene detected, double standard curves were established: one curve was made using the glyceraldehyde-3-phosphate-dehydrogenase (GAPDH) housekeeping gene (used to normalize the amount of cDNA present in each PCR experiment), while the other curve was made using gene-specific primers (Table 1). Real-time PCR was performed using an Mx3000P Real-Time PCR System (Genetimes Technology Inc.) as follows: 50 °C for 2 min (initial step), 95 °C for 5 min, then 40 cycles at 94 °C for 30 s, 53 °C for 1 min, and 72 °C for 30 s. Relative changes in gene-specific mRNA expression levels compared with the uninfected control and normalized against GAPDH were quantified by the $2^{-\Delta\Delta Ct}$ method [19] using the instrument settings.

Results

HP-PRRSV replication kinetics in PAM cells *in vitro*

The replication kinetics of HP-PRRSV in PAM cells were evaluated to identify the appropriate time point to test for changes in gene expression. Replication kinetics analysis showed that the viral copy number gradually increased from 0 to 48 hpi, reached its peak at 48 hpi, and then decreased over the period of 48 to 96 hpi (data not shown). Virally induced cytopathic effects were obvious in cultured PAM cells at 48 hpi, and these effects continuously increased in severity until 60 hpi, at which point the infected cells began detaching from the cell culture plates with increased frequency. Based on these results, we selected the 40 hpi time point for analysis to enable total RNA to be extracted from living PAM cells for SSH library construction just before the peak of viral infection at 48 hpi.

cDNA library construction and screening

During SSH library construction, each step was validated by PCR or agarose gel electrophoresis. Southern blotting was used to evaluate the 200 samples obtained from each of the forward- and reverse-subtracted libraries (Fig. 1); the positive and negative controls produced the expected results. From the 400 samples, 358 positive clones exhibiting a twofold or greater gray density value in comparison to the control were identified with ~90 % subtraction efficiency (358/400); 183 and 148 clones were derived from the forward and reverse subtraction library, respectively, and all positive clones were sequenced.

Gene annotation and assignment to categories of similar gene function

To identify the up- or down-regulated genes that were isolated by SSH screening, the 358 sequences were imported into GenBank to search for homology to known genes by BLAST analysis. Of the 183 clones from the forward subtraction library, 151 were identified by their homologous sequence, 15 matched EST sequences from unknown genes, and 17 did not match any homologous sequence. Of the 148 clones from the reverse subtraction library, 101 were identified by their homologous sequence, 39 matched EST sequences from unknown genes, and 12 did not match any homologous sequence.

The frequencies of the differentially expressed genes in the forward- and reverse-subtraction libraries were evaluated (Table 2) and were classified into eight categories by

Table 1 Primers used for real time RT-PCR detection of differentially expressed genes

Gene	Sequence (5′ → 3′)	Annealing temperature (°C)	Size of product (bp)
GAPDH	CCTTCATTGACCTCCACTAC	55	320
	GTTGTCATACTTCTCATGGTTC		
Transforming growth factor beta type 1 receptor (TGFBR1) gene	TCTAGTTTCATTGCTTTG	52	257
	AGCTCTCCCATATGGTCG		
Agouti signaling protein	GTTCCATCCATGTTGCTG	53	232
	GACCTGGCAATCCCACTC		
CC chemokine receptor genes	GTTAATGAGTCTGACTGG	53	216
	CATTTTCTTGGGCTGCTT		
Epidermal growth factor	CCACTCTTGGGCATGTAT	51	254
	TTTCTGGCTCATTTCACT		
Toll-like receptor gene	GTGGCGCAGTGGTTAACG	57	191
	CAGGCTAGGGGTTGAATC		
TCR-alpha/delta chain genes	TATTCCATGTTCCTGGAT	50	214
	GAGAGTTATGCCTCCTGC		
Mx1	CGAGGTACCAACTTACAT	51	240
	GGCAAAAGACCTGAATAG		
IL-8	AGCGTGGTCGCGGCCGAG	50	230
	GGCAGGTACAGAATAAAG		
Pig gender-neutral repetitive DNA	CAGTCAATCGGGATCCAT	55	229
	AGTGGATTTCATGCAGCG		
MHC class I SLA genes	ATATTCCCAGGGTTATGC	54	188
	TGAGCTGTGGTGTAGGTC		
IL-16	AGTTGCTGGAGTTCCCGT	57	214
	GTTCCCAGGCTAGGGGTC		
Adenylate kinase 3-like 1 (AK3L1)	AGGCTAGGGGTCGAATTG	54	243
	ACAGCAGCAAAAATTGAT		
Ferritin heavy polypeptide 1, FTH1	TGTCAAAGAGATACTCGG	53	232
	ACCGGAGCGCGATGACTG		
HSP70	AAGGCGTTCTACCCGGAGGAG	56	270
	ACCCAAGTCGAAAATGAGCAC		
Polyglutamine binding protein variant 4 (PQBP1 gene)	ACAATTCCACACAACATACGAG	56	206
	AGGGAGCGAGGAAGCGAAGAG		
MHC class II antigen (SLA-DRB1)	GTGGATGAGTTCAGATGCACAG	54	198
	TCCTCAGACTCTCCTTTGCTTC		
Skeletal muscle ryanodine receptor	GATTTACAAGGTTGTGATAATTTC	52	251
	CATCTCAGGTAACCCCTCCGTCTC		
Fibrinogen alpha chain preproprotein (FGA) gene	TTCCGTTCCATTTTAAAGCACCAC	55	236
	TGCTCCACCAGATAAGAATGAACC		
Mandelonitrile lyase	GAGTTCTTGGCTGAAGTTGATGTG	55	239
	TCTGAAGGTGGGAAAAGAAATG		
apaf1-like mRNA	ACCAGGCCAATGAGGTAGACTTCC	55	243
	TGACTGTGACACCCACATTCATTC		
Hepatoma-derived growth factor	CTTAATGTATTTTGGATATTAG	54	148
	CAATAGGCAAAAGGAATCACATC		

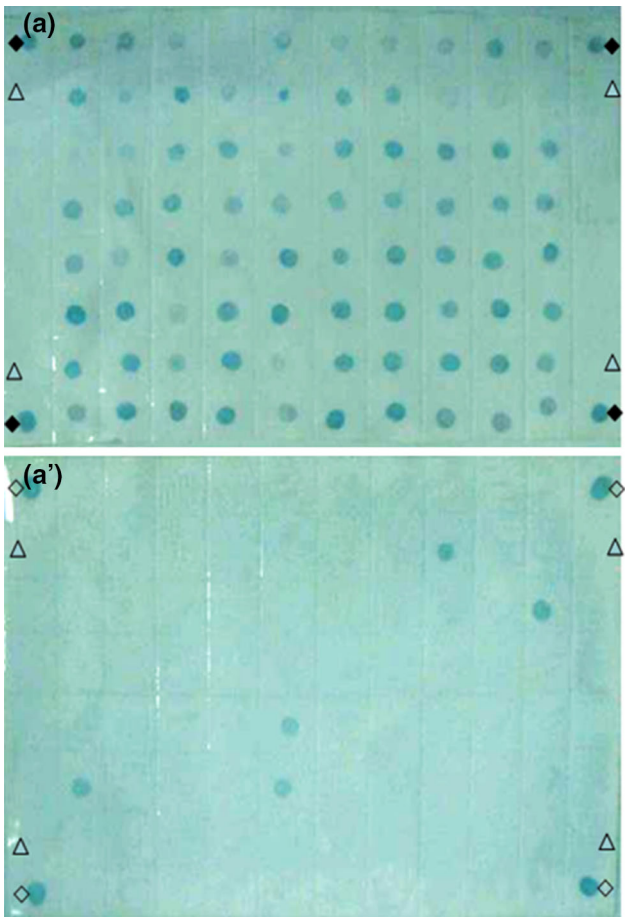

Fig. 1 Southern blot analysis of differentially expressed genes (partial genes). The denatured PCR products of differentially expressed genes were dotted in duplicate onto two pieces of nylon membrane at the same position. The membranes were analyzed using DIG-labeled cDNA probes from either the (a) forward or the reverse (a′) subtraction libraries. The unlabeled subtraction libraries that served as positive controls were dotted onto the four corners of the membrane (◆, or ◇, according to which DIG-labeled probe was used). The gp90 gene from the avian reticuloendotheliosis virus (REV) was used as a non-pig-derived negative control (△)

gene function: metabolic, immune-related, cell signaling, transcription/translation, cytoskeleton regulation, cell adhesion and migration, ribosomal proteins, apoptosis/cell proliferation/cell differentiation regulators, and other genes (Table 2). The proportion of genes in each category was also considered, and the immune, metabolic, and cell signaling gene categories together represented approximately 70 % of the differentially expressed genes within these top three gene families (Fig. 2a). After PRRSV HuN4 infection, 40 % of immune-related genes were upregulated in PAM cells; additionally, infection also induced expression of cell signaling, metabolic, and adhesion/migration genes (Fig. 2b). In contrast, PRRSV HuN4 infection downregulated genes related to ribosomal proteins, cytoskeleton regulation, and apoptosis/cell proliferation/cell differentiation (Fig. 2c).

IL-8 production is increased in PAM cells upon HP-PRRSV HuN4 infection

Because macrophages are capable of producing IL-8, using ELISA, we investigated whether PAMs were able to upregulate IL-8 production in response to HP-PRRSV HuN4 infection. Indeed, the IL-8 concentration was significantly higher than that of the uninfected control in PAM cells after infection ($p < 0.01$), reaching 1113 pg/mL at 48 hpi and 1437 pg/mL at 72 hpi (Fig. 3).

Expression of innate immune Mx1 and HSP70 antiviral proteins is increased in PRRSV-infected PAM cells

Expression of antiviral proteins known to be induced within macrophages under viral infection conditions was also analyzed by western blotting. mAbs targeting Mx1 or HSP70 were used to analyze protein expression over time in uninfected control cells or PRRSV-HuN4-infected PAM cells. Mx1 (72 kDa) was detected in uninfected PAM control cells and infected PAM cells, but its expression level increased upon PRRSV HuN4 infection (Fig. 4). Similarly, the HSP70 protein (70 kDa) expression level also increased after PRRSV infection. Although the expression levels of Mx1 and HSP70 showed a tendency to decrease at the late stage of infection, the expression level in the infected cells was higher than that in the uninfected control cells.

mRNA expression level changes of differentially expressed genes in PAM cells from HP-PRRSV infected piglets

To determine if similar patterns of gene expression were detectable in lung-resident PAM cells after *in vivo* infection with HP-PRRSV, we inoculated piglets with the PRRSV HuN4 strain and evaluated signs of infection in the piglets as well as gene expression levels in PAM cells harvested directly from the infected piglets at various time points after infection. Although all piglets had normal body temperatures before the experimental infections were administered, all infected piglets exhibited fever (40.5–41.6 °C) beginning at 2 dpi (Fig. 5a) and showed signs of anorexia, coughing, skin cyanopathy, shivering or lameness. One infected piglet died at 11 dpi, and the remaining piglets were euthanized at 14 dpi. Using quantitative RT-PCR analysis of the serum samples that were harvested, viremia was found to start at 3 dpi (Fig. 5b). Compared with the lungs from uninfected piglets (Fig. 5c), severe proliferative interstitial pneumonia and massive lymphomononuclear infiltration was evident in the lungs of infected piglets (Fig. 5d). These results showed that piglets

Table 2 Genes that were differentially expressed between uninfected PAM cells and those infected with HP-PRRSV strain HuN4. The genes were functionally classified according to DAVID bioinformatics resource [8, 13, 14]

Category	Number of clones	Identified gene	Sequence length	Percent sequence identity and GenBank accession number	Up (↑) or down (↓) regulation
Metabolic					
	1	GBA gene for putative lysosomal glucocerebrosidase precursor	447 bp	*Sus scrofa*, 95 % (215/224), AJ575650.1	↑
	20	Agouti signaling protein	442 bp	*Sus scrofa*, 90 % (275/303), AB206998.1	↑
	11	Adenylate kinase 3-like 1 (AK3L1)	996 bp	*Sus scrofa*, 91 % (235/258), EF488234	↑
	8	Mandelonitrile lyase	1227 bp	Lilium longiflorum, 100 % (30/30), DQ907931	↓
	4	Nitric oxide synthase	1228 bp	*Sus scrofa*, 81 % (162/200), AF535216.1	↓
	4	Guanylate binding protein 1 (GBP1)	1228 bp	*Sus scrofa*, 81 % (166/204), EU259886.1	↓
	4	Galactoside-binding, soluble, 1	618 bp	*Sus scrofa*, 99 % (364/365), NM001001867.1	↓
	2	Biotindase (BTD) gene	271 bp	*Homo sapiens*, 84 % (187/221), AF018631.1	↓
Immune related					
	6	Mx1	442 bp	*Sus scrofa*, 89 % (271/302), AB259856.1	↑
	15	Proliferation-inducing gene 15 (ferritin heavy polypeptide 1, FTH1)	351 bp	*Homo sapiens*, 85 % (263/309), XM001104405.1	↑
	31	T cell receptor alpha/delta chain gene	822 bp	*Sus scrofa*, 85 % (529/619), AB182374.1	↑
	2	IL-8	246 bp	*Sus scrofa*, 99 % (206/207), AB057440.1	↑
	1	IL-16	468 bp	*Sus scrofa*, 90 % (227/251), AB106555.1	↑
	15	MHC class I SLA genes	983 bp	*Sus scrofa*, 92 % (253/275), AJ251914	↑
	13	IFNAR1 gene, IFNGR2 gene and TMEM50B gene	490 bp	*Sus scrofa*, 95 % (244/256), AM229679.1	↑
	1	CD3 zeta chain gene	785 bp	*Sus scrofa*, 92 % (250/272), AB188402.1	↑
	21	CC chemokine receptor	705 bp	*Sus scrofa*, 93 % (242/258), AP006184.1	↑
	1	MHC class II antigen (SLA-DRB1) mRNA	454 bp	*Sus scrofa*, 100 % (118/118), DQ883227	↓
	1	Interleukin 2 receptor gamma	1225 bp	*Sus scrofa*, 81 % (211/258), AB092652.1	↓
	1	T cell receptor delta chain	521 bp	*Homo sapiens*, 100 % (51/51), AM408131.1	↓
Cell signaling					
	1	Tumor necrosis factor-like weak inducer of apoptosis (TWEAK)	369 bp	*Sus scrofa*, 86 % (237/275), EF624457.1	↑
	6	TRIM39, FLJ22638, GNL1, CAT56 genes	996 bp	*Sus scrofa*, 88 % (248/279), AB158488.1	↑
	10	TLR6, TLR1, TLR10 genes	735 bp	*Sus scrofa*, 95 % (281/293), AB210286.1	↑
	4	transforming growth factor beta type 1 receptor (TGFBR1) gene	828 bp	*Sus scrofa*, 97 % (768/789), DQ519377.1	↑

Table 2 continued

Category	Number of clones	Identified gene	Sequence length	Percent sequence identity and GenBank accession number	Up (↑) or down (↓) regulation
	1	RAG-1 gene for recombination-activating protein 1	447 bp	*Sus scrofa*, 95 % (214/223), AB091392.1	↑
	2	Pig alveolar macrophage-derived chemotactic factor-I (AMCF-I)	246 bp	*Sus scrofa*, 98 % (204/207), M99367.1	↑
	5	Protease serine 11 (IGF binding)	1202 bp	*Sus scrofa*, 94 % (605/643), AJ853849.1	↑
	15	Myostatin gene	423 bp	*Sus scrofa*, 96 % (371/384), AY208121.1	↑
	10	Ataxia-telangiectasia mutated protein	423 bp	*Sus scrofa*, 97 % (376/384), AY587061.1	↑
	3	apaf1-like mRNA	1218 bp	Danio rerio, 100 % (28/28), AM422109.1	↓
	2	Actin- related protein 2/3 complex, subunit 3 (Arpc3)	338 bp	*Homo sapiens*, 93 % (279/297), NM005719.2	↓
	2	TFF gene cluster for trefoil factor	443 bp	*Homo sapiens*, 80 % (76/95), AB038162.1	↓
	3	Fibrinogen alpha chain preproprotein (FGA) gene	1212 bp	*Homo sapiens*, 87 % (56/64), AF361104.1	↓
	1	PACSIN2	521 bp	*Homo sapiens*, 98 % (67/68), CR456536.1	↓
Transcription/translation					
	1	Eukaryotic translation elongation factor 1 alpha 1	864 bp	*Sus scrofa*, 99 % (821/826), NM001097418.1	↑
	1	Polyglutamine binding protein variant 4 (PQBP1 gene)	1188 bp	*Homo sapiens*, 95 % (429/450), AJ973596.1	↓
	1	Nuclear receptor subfamily 3, group C, member 2 (NR3C2)	1222 bp	*Homo sapiens*, 80 % (129/160), EU326312.1	↓
Cytoskeleton regulation					
	11	Skeletal muscle ryanodine receptor	693 bp	*Sus scrofa*, 83 % (144/172), X69465.1	↓
	2	p21-Arc	338 bp	*Homo sapiens*, 93 % (279/297), AF006086.1	↓
Cell adhesion and migration					
	3	Kirrel, cd1d genes for putative kin of IRRE-like protein, CD1D antigen	862 bp	*Sus scrofa*, 90 % (262/288), AB221036.1	↑
	6	ICAM3	735 bp	*Sus scrofa*, 95 % (281/294), AJ632303.1	↑
	15	Dopachrome tautomerase, glypican 6	1190 bp	*Sus scrofa*, 94 % (407/429), AB280947.1	↑
	3	Nitric oxide synthase	1207 bp	*Sus scrofa*, 81 % (162/199), DQ469808.1	↓
	2	Mucin 4 (MUC4)	693 bp	*Sus scrofa*, 91 % (92/101), DQ848681.1	↓
Ribosomal proteins					
	1	Ribosomal protein S28 (RPS28)	375 bp	*Sus scrofa*, 100 % (306/306), NM001001587.1	↓
	3	Ribosomal protein S19	253 bp	*Sus scrofa*, 98 % (226/229), AK233857.1	↓
	1	Ribosomal protein S17	472 bp	*Sus scrofa*, 100 % (391/391), NM001001634.1	↓

Table 2 continued

Category	Number of clones	Identified gene	Sequence length	Percent sequence identity and GenBank accession number	Up (↑) or down (↓) regulation
Apoptosis, cell proliferation, and cell differentiation regulators					
	2	Galactose-binding lectin	618 bp	*Sus scrofa*, 99 % (364/365), NM001001867.1	↓
Other proteins					
	1	Mitochondrial ATPase 6	285 bp	*Sus scrofa*, 99 % (112/113), AF250315.1	↑
	10	COX7A1, CAPNS1, CKAP1 genes	785 bp	*Sus scrofa*, 92 % (254/273), AJ410870.1	↑
	2	Olfactory receptor	828 bp	*Sus scrofa*, 97 % (768/790), AB221038.1	↑
	6	Epidermal growth factor	753 bp	*Sus scrofa*, 91 % (457/498), AF079769.1	↑
	12	Beta-casein (csn2) gene	502 bp	*Sus scrofa*, 97 % (232/238), EU213063.1	↑
	1	Adiponectin receptor 1 (ADIPOR1)	468 bp	*Sus scrofa*, 89 % (235/264), AY859427.1	↑
	1	Heat shock protein 70	541 bp	*Sus scrofa*, 99 % (497/501), X68213.1	↑
	1	Breed Chinese northeast wildboar mitochondrion	284 bp	*Sus scrofa*, 98 % (233/236), AK230489.1	↓

infected with the PRRSV HuN4 strain experienced the effects of severe illness.

From the differentially expressed genes that were identified in the *in vitro* infection experiment, we selected 21 representatives to test in the PAM cells harvested from the *in vivo* infections, including 14 upregulated and seven downregulated genes. mRNA expression of the 21 genes was analyzed by real-time PCR. Among the selected 14 upregulated genes, 13 were exposed at higher levels in PAM cells from the infected piglets than from the uninfected mock control at both 7 and 14 dpi; only ferritin heavy polypeptide 1 (FTH1) was reduced, which contrasts with the *in vitro* result. Quantitatively, the differentially expressed genes exhibited changes in the 1- to 5-fold range in the infected pigs compared with the uninfected controls (Fig. 6).

Among the seven downregulated genes, six were expressed at lower levels in PAMs from the infected piglets than in PAMs from uninfected piglets at 0 dpi; only the polyglutamine binding protein variant 4 (PQBP1) was higher than at 0 dpi. Specifically, Toll-like receptors, IL-16, TGF-beta type 1 receptor gene, agouti signaling protein gene, TCR-α/β chain gene, CC chemokine receptor gene, PQBP1, IL-8, epidermal growth factor gene, Ak3L1, MHC-I SLA genes, Mx1, and HSP70 were upregulated in the infected piglets compared with the uninfected control group ($p < 0.01$). Genes encoding the hepatoma-derived growth factor, skeletal muscle ryanodine receptor, apaf1-like mRNA, ferritin heavy polypeptide 1 (FTH1), fibrinogen alpha chain preproprotein (FGA) gene, mandelonitrile lyase, and MHC-II (SLA-DRB1) were downregulated ($p < 0.01$).

Discussion

In this study, we investigated changes in gene expression in PAMs in response to infection with HP-PRRSV to better understand the possible mechanism(s) underlying its enhanced infectivity and pathogenicity. Here, the expression profiles of genes in HP-PRRSV-HuN4-infected PAM cells were compared with their uninfected counterparts using the SSH method, and 358 clones were identified and verified by Southern blotting. Classification of these genes according to their biological functions revealed upregulated genes related to immune function (40 %) and cell signaling (24 %) and downregulated genes related to ribosomal proteins, cytoskeleton regulation, and apoptosis/cell differentiation in the HP-PRRSV-infected PAM cells.

Among the 21 differentially expressed genes in PAM cells harvested from piglets after *in vivo* HP-PRRSV infection that were selected to be analyzed by real-time RT-PCR, 19/21 (90.5 %) exhibited the same trends observed by Southern blot analysis of PAM cells infected *in vitro*. Specifically, 13 of the 14 genes that were upregulated *in vitro* were confirmed to increase, and 6 of the 7 downregulated genes were confirmed to decrease in PAM cells after *in vivo* HP-PRRSV infection. The finding that

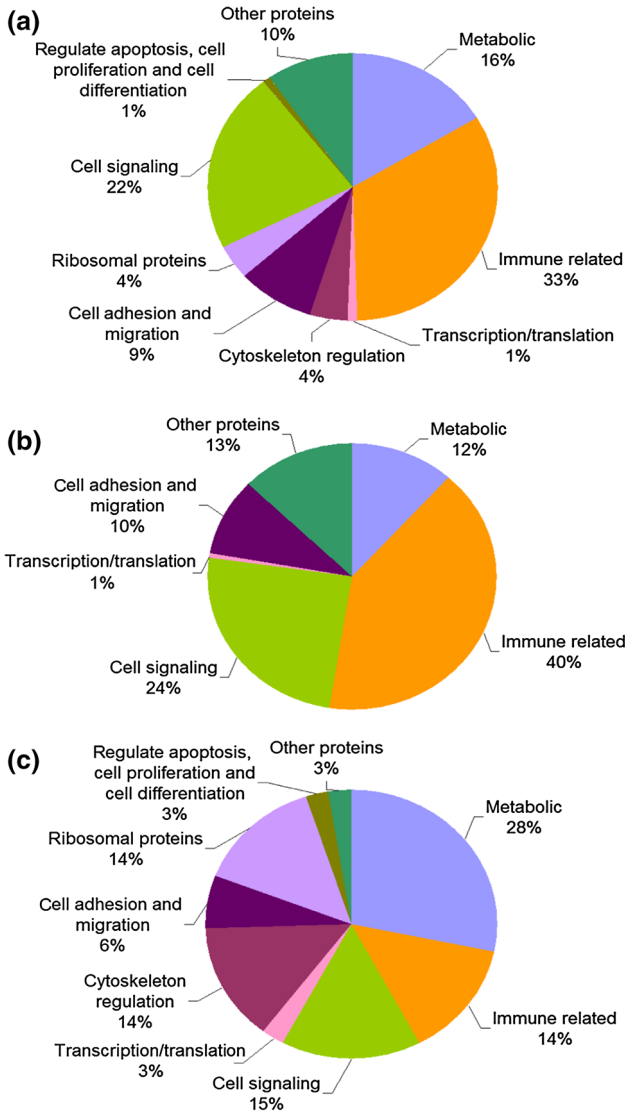

Fig. 2 Functional classification of differentially expressed genes. Genes were classified into eight groups based on their functional similarity, including metabolic, immune-related, cell signaling, transcription/translation, cytoskeleton regulation, cell adhesion and migration, ribosomal proteins, apoptosis/cell proliferation/cell differentiation regulation, and other genes. (a) Overall changes in the differentially expressed genes. Among the eight categories, the top three changes in gene expression were in the metabolic, immune-related, and cell signaling categories. (b) Upregulated genes. Among genes with upregulated expression, immune-related genes were the most common. Only five categories exhibited upregulated gene expression, excluding those whose function is unknown. (c) Downregulated genes. Among genes with downregulated expression, ribosomal, cytoskeleton, and apoptosis/cell differentiation genes were inhibited in PAM cells after infection with highly pathogenic PRRSV *in vitro*

two genes did not follow the same trend observed in the Southern blot analysis might result from differences between the *in vitro* and *in vivo* infections, such as the influence of other cell types or the time point after PRRSV infection that was chosen for testing.

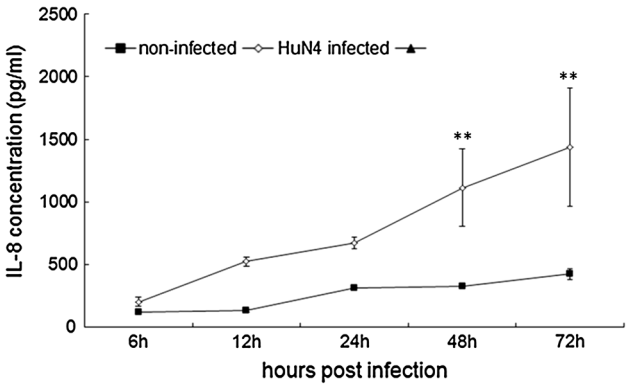

Fig. 3 IL-8 protein expression. PAM cells were infected with the highly pathogenic PRRSV HuN4 strain. Cell supernatants were collected and assayed using a commercial ELISA IL-8 kit. Data are expressed as the mean ± SD (n = 3). **, significant increase of IL-8 in HuN4-infected PAM cells compared with the uninfected control ($p < 0.01$)

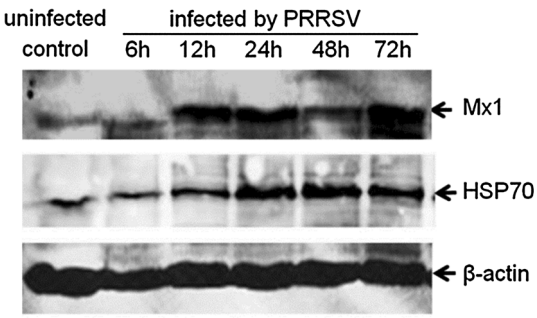

Fig. 4 Western blot analysis of Mx1 and HSP70 protein expression. PAM cells infected with 100 $TCID_{50}$ of PRRSV HuN4 were collected at 6, 12, 24, 48, and 72 hpi to analyze the changes in Mx1 and HSP70 protein expression under infection conditions. Compared with the uninfected control, Mx1 and HSP70 expression increased in the PRRSV-infected PAM cells. The molecular weights of Mx1, HSP70, and the β-actin loading control were 72 kDa, 70 kDa, and 42 kDa, respectively. hpi, hours postinfection

During the process of verifying protein expression of the differentially expressed genes, we confirmed that the representative proteins Mx1, HSP70 (by western blot), and IL-8 (by ELISA), were upregulated. Protein expression for most of the genes identified was not evaluated, because antibodies specifically recognizing these porcine proteins were not available. Mx1 protein, induced by antiviral type I IFNs, is responsible for mediating a specific antiviral state against influenza virus infection in murine [30] and porcine [29] hosts; it accumulates in the nucleus and inhibits influenza virus replication at the level of primary transcription [5]. In pigs, Mx1 expression was also found to be upregulated after PRRSV infection in a peptide-conjugated morpholino oligomer inhibition assay [28] as well as in foot-and-mouth disease virus (FMDV)-infected nasal mucosal epithelial cells *in vitro* and *in vivo*. Interestingly,

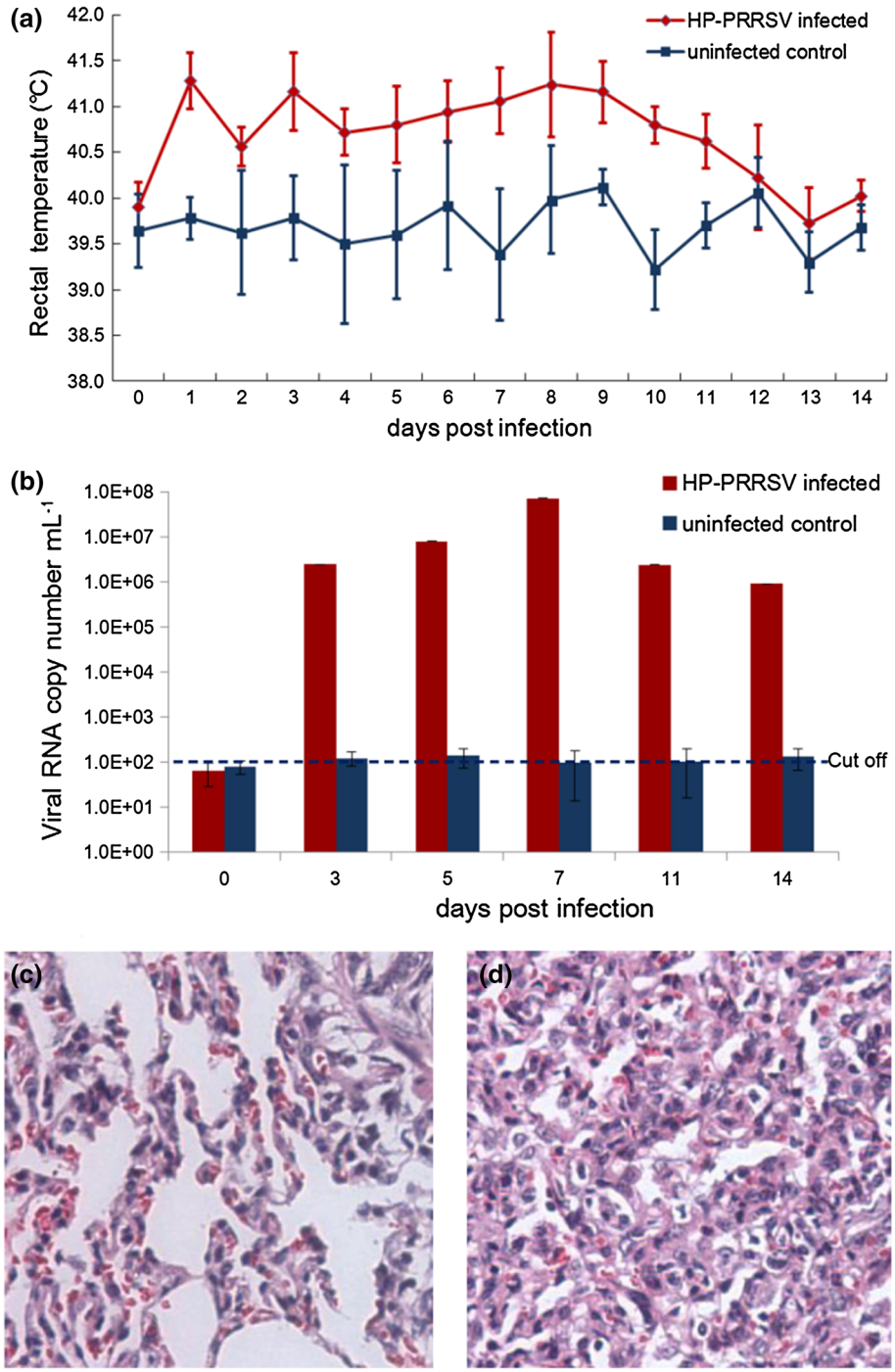

Fig. 5 Clinical and pathologic features of HP-PRRSV-infected and uninfected control piglets. (a) Mean rectal temperature (°C) of the piglets. (b) Mean PRRSV titers (expressed as viral RNA copies per mL) in serum estimated by real-time RT-PCR analysis. (c–d) Histopathological examination of lung tissue from an uninfected control (c) and an HP-PRRSV-infected pig (d) at 14 dpi. Lungs from HP-PRRSV-infected piglets displayed signs of robust interstitial pneumonia with thickening of the alveolar septa accompanied by extensive infiltration of lymphomononuclear cells. dpi, days postinfection

FMDV infection also induced IL-8 protein expression [7]. IL-8 and IFN-γ are linked to PRRS virus clearance [21]. IL-8, an important leukocyte chemokine, is produced by monocytes and macrophages and primarily functions in chemotaxis, inflammation, and neutrophil granulocyte activation. In the present study, expression of the inflammatory cytokine IL-16 and CC chemokine receptor genes (CCR3, CCR2, CCR5, and CCRL2) was also induced after PRRSV infection.

The real-time PCR results indicate that PRRSV infection triggers TCR-α/β, MHC class I, IL-8, IL-16, and Toll-like receptor expression and turns off MHC class II expression. MHC molecules are critical for antigen processing, management, and presentation, and TCR-α/β recognizes MHC molecules by their CDR1 and CDR2 domains. The data obtained in our study are consistent with the different functions of MHC class I and II molecules, because class II molecules mainly present exogenous

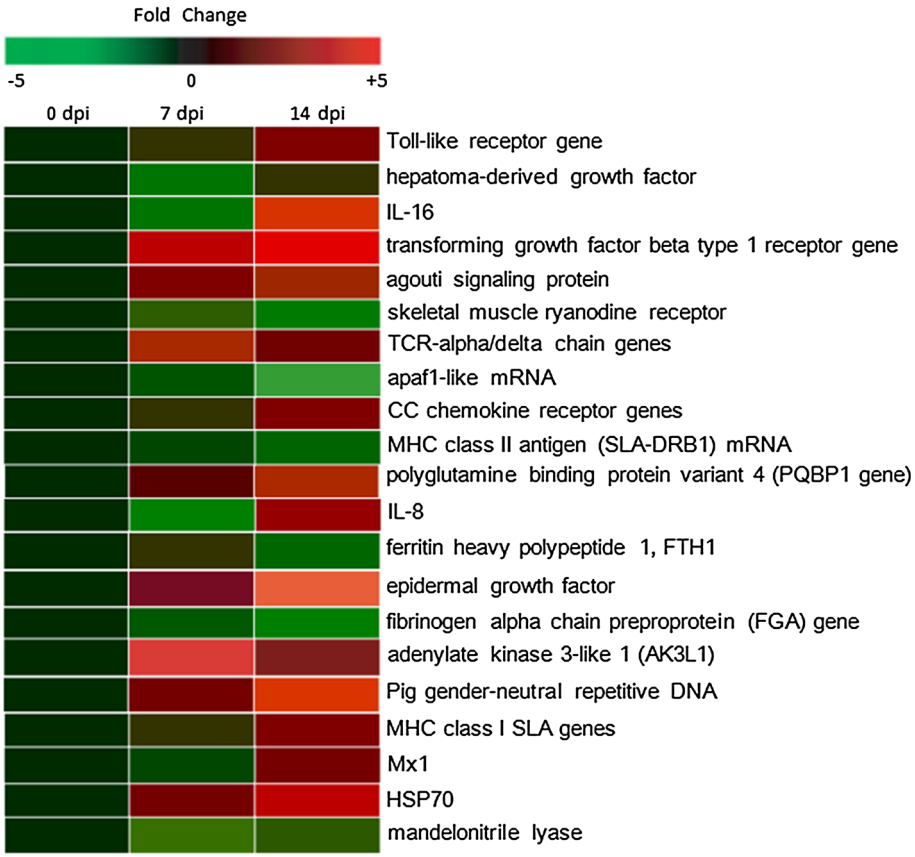

Fig. 6 mRNA expression levels of differentially expressed genes *in vivo* determined by quantitative real-time RT-PCR at 7 and 14 dpi. Data represent the average values from three animals. Up- or downregulated genes were detected together with the internal reference gene, GAPDH, which was used to normalize the amount of cDNA in each PCR experiment. Gene expression at 0 dpi was defined to be 1, and gene expression at 7 or 14 dpi was calculated relative to gene expression at 0 dpi. Thirteen out of 14 genes were confirmed to be upregulated, and 6 out of 7 genes were confirmed to be downregulated in PAM cells from infected piglets. Genes shown in red were upregulated, and those shown in green were downregulated in the infected piglets as compared with the uninfected controls. dpi, days postinfection

antigen to CD4 + T cells, while class I molecules present endogenous antigens to CD8+ cytotoxic T lymphocytes, and these cells are known to be required for viral clearance during viral infections.

Xiao et al. evaluated the lung response to either HP-PRRSV or classical North American PRRSV infection using whole lung tissue and found that an anti-apoptotic and anti-inflammatory state was induced to subvert the host innate immune response [39, 40]. Another recent study revealed that HP-PRRSV infection induced gene expression related to cytoskeleton and exocytosis organization, protein degradation and folding, intracellular calcium regulation, and zinc homeostasis in PAMs harvested from infected piglets [41]. However, no comprehensive study has been performed to investigate the innate immune changes induced specifically within PAMs upon infection with the highly pathogenic strain. SSH is a powerful technique for comparison of two mRNA populations and for obtaining genes exclusively expressed by one population. SSH has overcome the technical limitations of traditional subtraction methods requiring several rounds of hybridization and that are not well suited to identifying rare mRNAs. Furthermore, SSH has become widely used because of its simple operation, high efficiency, and low false-positive rate [2, 18, 24, 26].

The highly pathogenic 1918 Spanish influenza A virus has been suggested to have triggered aberrantly high and sustained expression of many of the above-mentioned innate immune response genes in humans, including pro-inflammatory cytokines and chemokines, which could have contributed to the virulence of this pathogenic virus [4, 15, 17, 20, 31]. Compared with the highly pathogenic 1918 influenza A virus, the clinical and pathological features of HP-PRRSV are quite similar, including the high viral titers caused by rapid viral replication, severe lung tissue damage (bleeding, immune cell infiltration), and high morbidity and mortality. Therefore, the data presented in the present study suggest that the highly pathogenic PRRSV variant may, to some degree, cause excessive stimulation of the innate immune response.

In summary, the results from this study reveal that the differential gene expression we observed between HP-PRRSV-infected PAM cells and uninfected PAM cells is mainly related to differences in cell signaling and innate immunity. The results also indicate that HP-PRRSV infection excessively stimulates innate immune response genes, including proinflammatory cytokines and chemokines. Further studies will be necessary to decipher the roles of the differentially expressed genes in HP-PRRSV infection that were identified in this study.

Acknowledgments This study was supported by grants from the National Natural Science Foundation of China (No. 30901080, 31270045) and the National Postdoctoral Science Foundation (Nos. 20090451026, 201003467). The authors thank Dr. Qing-Men Meng and Fu-Shan Tan for technical support with the Southern blotting experiments, and Sheng-Zhi Zhang for the real-time RT-PCR analyses.

Conflict of interest The authors declare that they have no conflict of interest.

References

1. An TQ, Tian ZJ, Leng CL, Peng JM, Tong GZ (2011) Highly pathogenic porcine reproductive and respiratory syndrome virus, Asia. Emerg Infect Dis 17(9):1782–1784
2. Bahn SC, Bae MS, Park YB, Oh SI, Jeung JU, Bae JM, Chung YS, Shin JS (2001) Molecular cloning and characterization of a novel low temperature-induced gene, blti2, from barley (*Hordeum vulgare* L.). Biochim Biophys Acta 1522:134–137
3. Cavanagh D (1997) Nidovirales: a new order comprising *Coronaviridae* and *Arteriviridae*. Arch Virol 142:629–633
4. Cheung CY, Poon LL, Lau AS, Luk W, Lau YL, Shortridge KF, Gordon S, Guan Y, Peiris JS (2002) Induction of proinflammatory cytokines in human macrophages by influenza A (H5N1) viruses: a mechanism for the unusual severity of human disease? Lancet 360:1831–1837
5. Cilloniz C, Pantin-Jackwood MJ, Ni C, Carter VS, Korth MJ, Swayne DE, Tumpey TM, Katze MG (2012) Molecular signatures associated with Mx1-mediated resistance to highly pathogenic influenza virus infection: mechanisms of survival. J Virol 86(5):2437–2446
6. Cline MS, Smoot M, Cerami E, Kuchinsky A, Landys N, Workman C, Christmas R, Avila-Campilo I, Creech M, Gross B, Hanspers K, Isserlin R, Kelley R, Killcoyne S, Lotia S, Maere S, Morris J, Ono K, Pavlovic V, Pico AR, Vailaya A, Wang PL, Adler A, Conklin BR, Hood L, Kuiper M, Sander C, Schmulevich I, Schwikowski B, Warner GJ, Ideker T, Bader GD (2007) Integration of biological networks and gene expression data using Cytoscape. Nat Protoc 2:2366–2382
7. Dash P, Barnett PV, Denyer MS, Jackson T, Stirling CM, Hawes PC, Simpson JL, Monaghan P, Takamatsu HH (2010) Foot-and-mouth disease virus replicates only transiently in well differentiated porcine nasal epithelial cells. J Virol 84(18):9149–9160
8. Dennis G Jr, Sherman BT, Hosack DA, Yang J, Gao W, Lane HC, Lempicki RA (2003) DAVID: Database for Annotation, Visualization, and Integrated Discovery. Genome Biol 4:P3
9. Duan X, Nauwynck H, Pensaert M (1997) Effects of origin and state of differentiation and activation of monocytes/macrophages on their susceptibility to PRRSV. Arch Virol 142:2483–2497
10. Genini S, Delputte PL, Malinverni R, Cecere M, Stella A, Nauwynck HJ, Giuffra E (2008) Genome-wide transcriptional response of primary alveolar macrophages following infection with porcine reproductive and respiratory syndrome virus. J Gen Virol 89:2550–2564
11. Gracey AY, Troll JV, Somero GN (2001) Hypoxia-induced gene expression profiling in the euryoxic fish Gillichthys mirabilis. Proc Natl Acad Sci USA 98(4):1993–1998
12. Guo BQ, Chen ZS, Liu WX, Cui YZ (1996) Isolation and identification of porcine reproductive and respiratory syndrome (PRRS) virus from aborted fetuses suspected of PRRS. Chin J Infect Diseases Anim Poult 18:1–5 (in Chinese)
13. Huang DW, Sherman BT, Lempicki RA (2009) Bioinformatics enrichment tools: paths toward the comprehensive functional analysis of large gene lists. Nucleic Acids Res 37(1):1–13
14. Huang DW, Sherman BT, Lempicki RA (2009) Systematic and integrative analysis of large gene lists using DAVID Bioinformatics Resources. Nat Protoc 4(1):44–57
15. Kash JC, Tumpey TM, Proll SC, Carter V, Perwitasari O, Thomas MJ, Basler CF, Palese P, Taubenberger JK, García-Sastre A, Swayne DE, Katze MG (2006) Genomic analysis of increased host immune and cell death responses induced by 1918 influenza virus. Nature 443(7111):578–581
16. Keffaber KK (1989) Reproductive failure of unknown etiology. Am Assoc Swine Pract Newslett 1:1–10
17. Kobasa D, Jones SM, Shinya K, Kash JC, Copps J (2007) Aberrant innate immune response in lethal infection of macaques with the 1918 influenza virus. Nature 445(7125):319–323
18. Lavoie JP, Lefebvre-Lavoie J, Leclere M, Lavoie-Lamoureux A, Chamberland A, Laprise C, Lussier J (2012) Profiling of differentially expressed genes using suppression subtractive hybridization in an equine model of chronic asthma. PLoS ONE 7(1):e29440
19. Livak KJ, Schmittgen TD (2001) Analysis of relative gene expression data us-ing real-time quantitative PCR and the 2(−Delta Delta C(T)) method. Methods 25(4):402–408
20. Loo YM, Gale M Jr (2007) Fatal immunity and the 1918 virus. Nature 445(7125):267–268
21. Lunney JK, Fritz ER, Reecy JM, Kuhar D, Prucnal E, Molina R, Christopher-Hennings J, Zimmerman J, Rowland RR (2010) Interleukin-8, interleukin-1beta, and interferon-gamma levels are linked to PRRS virus clearance. Viral Immunol 23(2):127–134
22. Meulenberg JJ, Hulst MM, de Meijer EJ, Moonen PL, den Besten A, de Kluyver EP, Wensvoort G, Moormann RJ (1993) Lelystad virus, the causative agent of porcine epidemic abortion and respiratory syndrome (PEARS), is related to LDV and EAV. Virology 192(1):62–72
23. Meulenberg JJ, Hulst MM, de Meijer EJ, Moonen PL, den Besten A, de Kluyver EP, Wensvoort G, Moormann RJ (1994) Lelystad virus belongs to a new virus family, comprising lactate dehydrogenase-elevating virus, equine arteritis virus, and simian hemorrhagic fever virus. Arch Virol 9:441–448
24. Mikami Y, Somei M, Takagi M (2009) A new synthetic compound, SST-VEDI-1, inhibits osteoblast differentiation with a down-regulation of the Osterix expression. J Biochem 145(2):239–247
25. Miller LC, Neill JD, Harhay GP, Lager KM, Laegreid WW, Kehrli ME Jr (2010) In-depth global analysis of transcript abundance levels in porcine alveolar macrophages following infection with porcine reproductive and respiratory syndrome virus. Adv Virol 864181:2010. doi:10.1155//864181
26. Monteiro RA, Balsanelli E, Tuleski T, Faoro H, Cruz LM, Wassem R, de Baura VA, Tadra-Sfeir MZ, Weiss V, DaRocha WD, Muller-Santos M, Chubatsu LS, Huergo LF, Pedrosa FO, de Souza EM (2012) Genomic comparison of the endophyte *Herbaspirillum seropedicae* SmR1 and the phytopathogen *Herbaspirillum rubrisubalbicans* M1 by suppressive subtractive hybridization and partial genome sequencing. FEMS Microbiol Ecol 80(2):441–451
27. Nelsen CJ, Murtaugh MP, Faaberg KS (1999) Porcine reproductive and respiratory syndrome virus comparison: divergent evolution on two continents. J Virol 73:270–280
28. Opriessnig T, Patel D, Wang R, Halbur PG, Meng XJ, Stein DA, Zhang YJ (2011) Inhibition of porcine reproductive and respiratory syndrome virus infection in piglets by a peptide-conjugated morpholino oligomer. Antiviral Res 91(1):36–42

29. Palm M, Garigliany MM, Cornet F, Desmecht D (2010) Interferon-induced *Sus scrofa* Mx1 blocks endocytic traffic of incoming influenza A virus particles. Vet Res 41(3):29
30. Pavlovic J, Haller O, Staeheli P (1992) Human and mouse Mx proteins inhibit different steps of the influenza virus multiplication cycle. J Virol 66(4):2564–2569
31. Perrone LA, Plowden JK, García-Sastre A, Katz JM, Tumpey TM (2008) H5N1 and 1918 pandemic influenza virus infection results in early and excessive infiltration of macrophages and neutrophils in the lungs of mice. PLoS Pathog 4(8):e1000115
32. Snijder EJ, Meulenberg JJ (1998) The molecular biology of arteriviruses. J Gen Virol 79(Pt 5):961–979
33. Snijder EJ, van Tol H, Pedersen KW, Raamsman MJ, de Vries AA (1999) Identification of a novel structural protein of arteriviruses. J Virol 73(8):6335–6345
34. Tian K, Yu X, Zhao T, Feng Y, Cao Z, Wang C, Hu Y, Chen X, Hu D, Tian X, Liu D, Zhang S, Deng X, Ding Y, Yang L, Zhang Y, Xiao H, Qiao M, Wang B, Hou L, Wang X, Yang X, Kang L, Sun M, Jin P, Wang S, Kitamura Y, Yan J, Gao GF (2007) Emergence of fatal PRRSV variants: unparalleled outbreaks of atypical PRRS in China and molecular dissection of the unique hallmark. PLoS ONE 2:e526
35. Tong GZ, Zhou YJ, Hao XF, Tian ZJ, An TQ, Qiu HJ (2007) Highly pathogenic porcine reproductive and respiratory syndrome, China. Emerg Infect Dis 13(9):1434–1436
36. Voicu IL, Silim A, Morin M, Elazhary MA (1994) Interaction of porcine reproductive and respiratory syndrome virus with swine monocytes. Vet Rec 134:422–423
37. Wensvoort G, Wensvoort G, Terpstra C, Pol JM, ter Laak EA, Bloemraad M, de Kluyver EP, Kragten C, van Buiten L, den Besten A, Wagenaar F (1991) Mystery swine disease in the Netherlands: the isolation of Lelystad virus. Vet Q 13:121–130
38. Wu WH, Fang Y, Farwell R, Steffen-Bien M, Rowland RR, Christopher-Hennings J, Nelson EA (2001) A 10-kDa structural protein of porcine reproductive and respiratory syndrome virus encoded by ORF2b. Virology 287(1):183–191
39. Xiao S, Jia J, Mo D, Wang Q, Qin L, He Z, Zhao X, Huang Y, Li A, Yu J, Niu Y, Liu X, Chen Y (2010) Understanding PRRSV infection in porcine lung based on genome-wide transcriptome response identified by deep sequencing. PLoS ONE 5(6):e11377
40. Xiao S, Mo D, Wang Q, Jia J, Qin L, Yu X, Niu Y, Zhao X, Liu X, Chen Y (2010) Aberrant host immune response induced by highly virulent PRRSV identified by digital gene expression tag profiling. BMC Genomics 11:544
41. Zhou P, Zhai S, Zhou X, Lin P, Jiang T, Hu X, Jiang Y, Wu B, Zhang Q, Xu X, Li JP, Liu B (2011) Molecular characterization of transcriptome-wide interactions between highly pathogenic porcine reproductive and respiratory syndrome virus and porcine alveolar macrophages in vivo. Int J Biol Sci 7(7):947–959